

Mechanical Stabilisation of Retained Austenite in δ -TRIP Steel

H. L. Yi^a, K. Y. Lee^b, H. K. D. H. Bhadeshia^{a,c}

^a*Graduate Institute of Ferrous Technology, Pohang University of Science and
Technology, Pohang 790-784, Republic of Korea*

^b*POSCO Technical Research Laboratories, Gwangyang-si, Jeonnam, Republic of Korea*

^c*Materials Science and Metallurgy, University of Cambridge, Cambridge CB2 3QZ, U.K.*

Abstract

Recent research suggests that extraordinary combinations of strength and ductility can be achieved in the so-called δ -TRIP steels, which contain ferrite, bainite and austenite. A part of the reason for the ductility of almost 40% elongation at a strength of some 900 MPa, is believed to be the optimal stability of the austenite to plastic deformation. We demonstrate here that mechanical stabilisation plays an important role in preserving the austenite to large plastic strains.

Keywords: TRIP-assisted steel, δ -TRIP, Mechanical stabilisation, Retained austenite

1. Introduction

TRIP-assisted steels, in which the retained austenite undergoes stress or strain-induced transformation into martensite gain tensile ductility because of the associated work hardening, which is responsible for delaying the onset of plastic instability [1–5]. ‘TRIP’ stands for transformation induced plasticity [6] but it is important to realise that the transformation strains themselves are a minor component of the total observed elongation [7]. There have been investigations which suggest that there is an optimum stability necessary for the retained austenite [8–10]. If it decomposes during the early stages of

Email addresses: hityih1@postech.ac.kr (H. L. Yi), (K. Y. Lee),
hkdb@cam.ac.uk, corresponding author (H. K. D. H. Bhadeshia)

deformation then it is not able to contribute when significant damage mechanisms initiate. Too high a stability in turn reduces its ability to enhance the work hardening capacity.

The stability of the retained austenite has in the past been considered in terms of two main factors, its chemical composition (primarily the carbon content) [10–12] or its size [13–23]. We show in this work that there is a further contribution, arising from the accumulation of deformation induced defects within the retained austenite, which resist the progress of martensitic transformation by a process known as *mechanical stabilisation* [13, 24–29].

2. Experimental

The alloy design procedure is described elsewhere [30], but was manufactured as a 34 kg ingot with dimensions $100 \times 170 \times 230$ mm using a vacuum furnace. The ingot was reheated to 1200°C for rough rolling to make 25–30 mm slabs followed by air cooling. The slabs were then reheated to 1200°C and hot-rolled with the temperature maintained above 900°C down to 3 mm thickness, followed by cold-rolling to 1.8 mm thick sheet. The final chemical compositions is as follows:



Tensile specimens (ASTM E8M-00) made from the alloy were intercritically annealed at 800°C for 10 min, cooled rapidly by quenching into a salt bath for isothermal transformation at 330°C for 30 min in order to induce the formation of bainitic ferrite; the samples were then air cooled to ambient temperature. The amount of retained austenite and bainitic ferrite in the final microstructure represents the fraction of austenite present at the intercritical annealing temperature; this fraction was found using quantitative metallography to be 0.43 ± 0.04 where the uncertainty represents one standard deviation.

The 1.8 mm thick tensile specimens were strained at $3.3 \times 10^{-3} \text{ s}^{-1}$, with the reported elongations measured over a gauge length of 10 mm. In one case, a tensile sample was, after fracture, subjected to X-ray diffraction at four locations on its length; the locations concerned were separated using an Accutom 50 precision cutter equipped with a 0.5 mm thick alumina cutting disc.

3. Mechanical behaviour and microstructure

Tensile testing revealed that the alloy has an excellent combination of ultimate tensile strength and elongation, with the product of these two quantities coming to $\approx 33,000$ MPa %; data from three such tests are summarised in Table 1 and all three true-stress versus true-strain curves are shown in Fig. 1 in order to illustrate the consistency of strain hardening rates between the specimens. Fig. 3 shows scanning electron micrographs of the structure before and after tensile deformation in the vicinity of the fracture position. The initial structure consists of allotriomorphic ferrite, and equiaxed, blocky regions of retained austenite containing plates of bainitic ferrite which in some cases partition the austenite into films. Fig. 3b shows the remarkable elongation of the austenite islands along the tensile axis; there is no sign of microcracking, which is surprising if the majority of the austenite has transformed into high carbon, untempered martensite.

X-ray experiments interpreted using Reitveld analysis revealed $19.6 \pm 0.2\%$ retained austenite in the initial structure; the carbon concentration (w_C) of the austenite was estimated from the lattice parameter (a_γ in Å) using the relationship due to Dyson and Holmes [31]:

$$\frac{w_C}{0.003} = a_\gamma - 3.578 - 0.00095w_{\text{Mn}} - 0.0056w_{\text{Al}} - 0.0015w_{\text{Cu}} \quad (1)$$

where w stands for the weight percent of the solute identified in the subscript. The concentration of the substitutional solutes specifically in the austenite was measured using energy dispersive X-ray microanalysis (Table 2). A reasonable average value of $w_C \approx 1.33$ wt% was obtained.

Fig. 2 shows that although the austenite does undergo some martensitic transformation during deformation, much of it is retained even at a distance less than about 2 mm away from the point of fracture. This is remarkable given that the plastic elongation recorded over a gauge length of 10 mm is in excess of 37%. In this respect, a re-examination of Fig. 3b shows that the larger blocky regions of austenite seem to have to some extent retained their shape whereas those which are subdivided by bainite plates have elongated. This would be consistent with the well-known effect that blocks of retained austenite are less stable than films [20]. We now proceed to explain why the austenite is reluctant to transform in spite of the large plastic strains involved.

4. Mechanical stabilisation of retained austenite

Martensitic transformation involves the glide of glissile α'/γ interfaces which consist of arrays of dislocations which can move without diffusion. The process is similar to conservative slip except that the structure of the interface leads to a change in crystal structure as it translates into the austenite [32]. Any obstacles in the path of the interface therefore hinder its motion, precisely in the same manner that slip dislocations are hindered by barriers such as forest dislocations. There comes a point where the density of barriers present in the austenite becomes so large that the driving force for the growth of martensite becomes inadequate compared with that which obstructs the interface. This defines the onset of mechanical stabilisation whence martensitic transformation ceases. This concept forms the basis of a quantitative model for predicting mechanical stabilisation when displacive transformations occur in austenite which is plastically deformed.

Mechanical stabilisation occurs when the stress driving (τ_T) the interface equals that opposing its motion, $\tau + \tau_S$, where τ is the resistance from dislocation debris in the austenite, and τ_S the contribution from solid-solution strengthening of austenite [33]:

$$\begin{aligned} \tau_T &= \tau + \tau_S \\ \text{so that } b\Delta G &= \frac{1}{8\pi(1-\nu)}Gb^{\frac{3}{2}}\sqrt{\frac{\epsilon}{L}} + \tau_S b \end{aligned} \quad (2)$$

where ϵ is the plastic strain, b is the magnitude of the Burgers vector of the dislocations involved, ΔG is the free energy change driving the motion of the interface, G is the shear modulus of the austenite and ν is its Poisson's ratio. L is the average distance moved by the dislocations and $L = \delta D/(\delta + D\epsilon)$ where D is the original grain size of austenite before straining, and δ is a coefficient equal approximately to $1 \mu m$ [34].

The original model considered transformation from deformed austenite which was not otherwise under the influence of an external stress. The present work involves tensile deformation so it is appropriate to include a mechanical free energy contribution to the driving force for martensitic transformation, and as in the earlier work, to reduce the total chemical free energy available by the stored energy of martensite (600 J mol^{-1} , [35]):

$$\Delta G = \Delta G_{\text{CHEM}} + \Delta G_{\text{MECH}} - 600 \text{ J mol}^{-1} \quad (3)$$

The chemical driving force for transformation, $\Delta G_{\text{CHEM}} = \Delta G_{\gamma} - \Delta G_{\alpha}$ was calculated using MTDATA combined with TCFE (1.21 version) database [36] at 20 °C, assuming the chemical composition of the austenite as listed in Table 2 and for two different carbon concentrations (1.2 and 1.4 wt%) rather than the average 1.33 wt% determined from the X-ray experiments. This is because larger regions of austenite are expected to contain relatively less carbon [11].

The mechanical component of the free energy change is given by $\Delta G_{\text{MECH}} = \sigma \times 0.86 \text{ J mol}^{-1}$ [37, 38], where σ is the external stress experienced by the austenite. The complete set of parameters used in the calculations is listed in Table 3.

Fig. 4 shows the calculations of the critical value of true strain required to trigger mechanical stabilisation, as a function of the maximum value of the true tensile stress experienced by the retained austenite. The stress assists martensitic transformation which means that mechanical stabilisation is triggered at ever larger values of the critical strain as the stress increases. The two curves represent two different carbon concentrations, the lower value assumed to be that corresponding to the blocks of austenite and the 1.4 wt% representing the film type austenite. They also differ in their grain sizes as listed in Table 3. The critical strain is zero, *i.e.*, transformation simply does not occur, if the stress is less than 1096 MPa in the case of the 1.2 wt% austenite, and 1631 MPa for the 1.4 wt% austenite.

The dashed vertical line represents the actual true stress to which the austenite is subjected for the tensile test data listed in Table 1, suggesting that mechanical stabilisation occurs when the austenite is deformed to a true strain of 13%; this corresponds to an engineering strain of about 14%, which is much smaller than the total elongation of 37%. This means that the austenite can transform only during the period of the initial strain, after which it becomes stabilised. The data presented in Fig. 2 support this conclusion. Furthermore, it is only the blocky austenite which is presumed to be leaner in carbon that can undergo transformation, consistent with the fact that the blocks show less elongation in micrographs than the film type austenite (Fig. 3). They would essentially cease to deform once hard, untempered, high-carbon martensite forms.

The implications of this interpretation are interesting, that the initial transformation helps enhance the work hardening capacity, but further ductility is maintained by austenite which deforms in a way that is approximately compatible with the overall microstructure. Indeed, Fig. 5 shows the stress–

strain relationship for one of the samples confirms that the work hardening rate diminishes significantly as the critical strain of 14% is approached.

5. Conclusions

A TRIP-assisted steel which exhibits substantial ductility contains austenite, the coarser regions of which transform during the early stages of deformation but the remainder is in a state which is mechanically stabilised and hence remains untransformed until the point of fracture. Thus, regions of austenite can be observed to elongate with the majority phase which is ferrite. A published theory for the mechanical stabilisation of the austenite has been adapted to provide a quantitative basis for assessing the onset of mechanical stabilisation when the austenite is not only contains deformation debris but is also under a state of mechanical stress.

Acknowledgments

We are grateful to Professor Hae-Geon Lee for laboratory facilities at GIFT, and to POSCO for the Steel Innovation Programme. Support from the World Class University Programme of the National Research Foundation of Korea, Ministry of Education, Science and Technology, project number R32-2008-000-10147-0 is gratefully acknowledged.

References

- [1] O. Matsumura, Y. Sakuma, H. Takechi: Transactions of the Iron and Steel Institute of Japan 27 (1987) 570–579.
- [2] O. Matsumura, Y. Sakuma, H. Takechi: Scripta Metallurgica 27 (1987) 1301–1306.
- [3] Y. Sakuma, O. Matsumura, H. Takechi: Metallurgical & Materials Transactions A 22 (1991) 489–498.
- [4] P. J. Jacques: Current Opinion in Solid State and Materials Science 8 (2004) 259–265.
- [5] B. DeCooman: Current Opinion in Solid State and Materials Science 8 (2004) 285–303.

- [6] W. W. Gerberich, G. Thomas, E. R. Parker, V. F. Zackay: Metastable austenites: decomposition and strength: in: Second International Conference on Strength of Metals and Alloys: ASM International, Ohio, USA, 1970: pp. 894–899.
- [7] H. K. D. H. Bhadeshia: *ISIJ International* 42 (2002) 1059–1060.
- [8] K. Sugimoto, N. Usui, M. Kobayashi, S. Hashimoto: *ISIJ International* 32 (1992) 1311–1318.
- [9] K. Sugimoto, M. Kobayashi, S. Hashimoto: *Metallurgical Transactions A* 23A (1992) 3085–3091.
- [10] C. Garcia-Mateo, F. G. Caballero: *Materials Transactions* 46 (2005) 1839–1846.
- [11] A. Itami, M. Takahashi, K. Ushioda: *ISIJ International* 35 (1995) 1121–1127.
- [12] Y. Sakuma, O. Matsumura, O. Akisue: *ISIJ International* 31 (1991) 1348–1353.
- [13] W. C. Leslie, R. L. Miller: *ASM Transactions Quarterly* 57 (1964) 972–979.
- [14] D. Duchateau, M. Guttman: *Acta Metallurgica* 29 (1981) 1291–1297.
- [15] M. Umemoto, W. S. Owen: *Metallurgical Transactions* 5 (1974) 2041–2046.
- [16] G. S. Ansell, P. J. Brofman, T. J. Nichol, G. Judd: Effect of austenite strength on the transformation to martensite in Fe–Ni and Fe–Ni–C alloys: in: G. B. Olson, M. Cohen (Eds.), *International Conference on Martensitic Transformations ICOMAT '79*: 1979: pp. 350–355.
- [17] P. J. Brofman, G. S. Ansell: *Metallurgical Transactions A* 14A (1983) 1929–1931.
- [18] S. J. Lee, Y. K. Lee: *Materials Science Forum* 475–479 (2005) 3169–3172.

- [19] J. Huang, Z. Xu: *Materials Science & Engineering A* A438–440 (2006) 254–257.
- [20] H. K. D. H. Bhadeshia, D. V. Edmonds: *Metal Science* 17 (1983) 411–419.
- [21] H. K. D. H. Bhadeshia, D. V. Edmonds: *Metal Science* 17 (1983) 420–425.
- [22] B. V. N. Rao, M. S. Rashid: *Metallography* 16 (1983) 19–37.
- [23] F. G. Caballero, C. G. Mateo, J. Chao, M. J. Santofimia, C. Capdevila, C. G. de Andrés: *ISIJ International* 48 (2008) 1256–1262.
- [24] E. S. Machlin, M. Cohen: *Trans. Metall. Soc. AIME* 191 (1951) 746–754.
- [25] H. C. Fiedler, B. L. Averbach, M. Cohen: *Transactions of the American Society for Metals* 47 (1955) 267–290.
- [26] J. R. Strife, M. J. Carr, G. S. Ansell: *Metallurgical Transactions A* 8A (1977) 1471–1484.
- [27] V. Raghavan: *Kinetics of Martensitic Transformations*: eds G. B. Olson and W. S. Owen, ASM International, Ohio, US, 1992: Ch. 11: pp. 197–226.
- [28] K. Tsuzaki, S. Fukasaku, Y. Tomota, T. Maki: *Trans. JIM* 32 (1991) 222–228.
- [29] H. K. D. H. Bhadeshia: *Materials Science & Engineering A* 273–275 (1999) 58–66.
- [30] H. L. Yi, K. Y. Lee, H. K. D. H. Bhadeshia: *Proceedings of the Royal Society A* 467 (2010) 234–243.
- [31] D. J. Dyson, B. Holmes: *Journal of the Iron and Steel Institute* 208 (1970) 469–474.
- [32] J. W. Christian: *Theory of Transformations in Metal and Alloys, Part II*: 3rd Edition: Pergamon Press, 2003.
- [33] S. Chatterjee, H. S. Wang, J. R. Yang, H. K. D. H. Bhadeshia: *Materials Science and Technology* 22 (2006) 641–644.

- [34] F. Barlat, M. V. Glazov, J. C. Brem, D. J. Lege: Canadian Metallurgical Quarterly 18 (2002) 919–939.
- [35] J. W. Christian: Thermodynamics and kinetics of martensite: in: G. B. Olson, M. Cohen (Eds.), International Conference on Martensitic Transformations ICOMAT '79: 1979: pp. 220–234.
- [36] NPL: MTDATA: Software, National Physical Laboratory, Teddington, U.K. (2006).
- [37] S. Denis, E. Gautier, A. Simon, G. Beck: Materials Science and Technology 1 (1985) 805–814.
- [38] G. B. Olson: Transformation plasticity and the stability of plastic flow: in: Deformation, Processing and Structure: American Society for Metals, Metals Park, Ohio, USA, 1982: pp. 390–424.

Table 1: The results of three tensile tests. The terms YS, UTS and TEL stand for yield strength, ultimate tensile strength and total elongation, respectively.

YS /MPa	UTS /MPa	UEL /%	TEL /%	UTS \times TEL / MPa%
573	882	31	38	33,247
541	880	31	37	32,940
536	894	31	37	32,691

Table 2: Alloying element distribution in phases in heat-treated specimens, wt%.

Phase	Al	Si	Mn	Cu
γ	2.56 \pm 0.14	0.32 \pm 0.08	1.87 \pm 0.17	0.55 \pm 0.13
α	3.13 \pm 0.05	0.40 \pm 0.06	1.15 \pm 0.05	0.44 \pm 0.06

Table 3: Parameters used for the modelling in blocky and lath type of austenite.

	D / m	C / wt%	G / Pa	ν	b / m	$\tau_s b /$ N m ⁻¹	ΔG_{Chem} / J mol ⁻¹
Blocky	5 \times 10 ⁻⁶	1.2	8 \times 10 ¹⁰	0.27	2.52 \times 10 ⁻¹⁰	0.057640	1281
Film	0.5 \times 10 ⁻⁶	1.4	8 \times 10 ¹⁰	0.27	2.52 \times 10 ⁻¹⁰	0.06644	1080

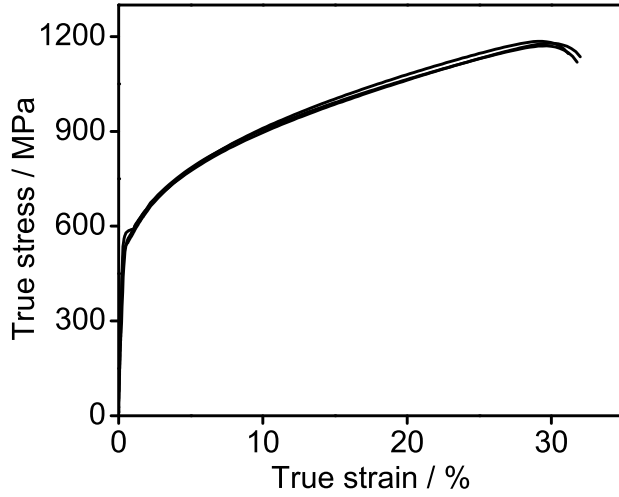


Figure 1: Superimposed true-stress versus true-strain curves for the three tensile tests.

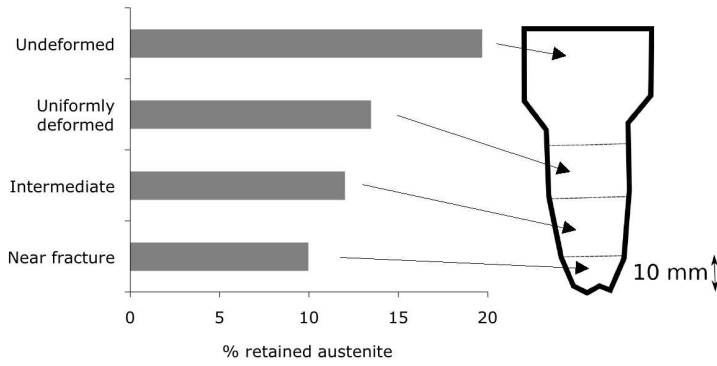


Figure 2: Retained austenite in different regions relative to the fracture surface. The point marked 'Fracture' is within 2 mm of the fracture surface.

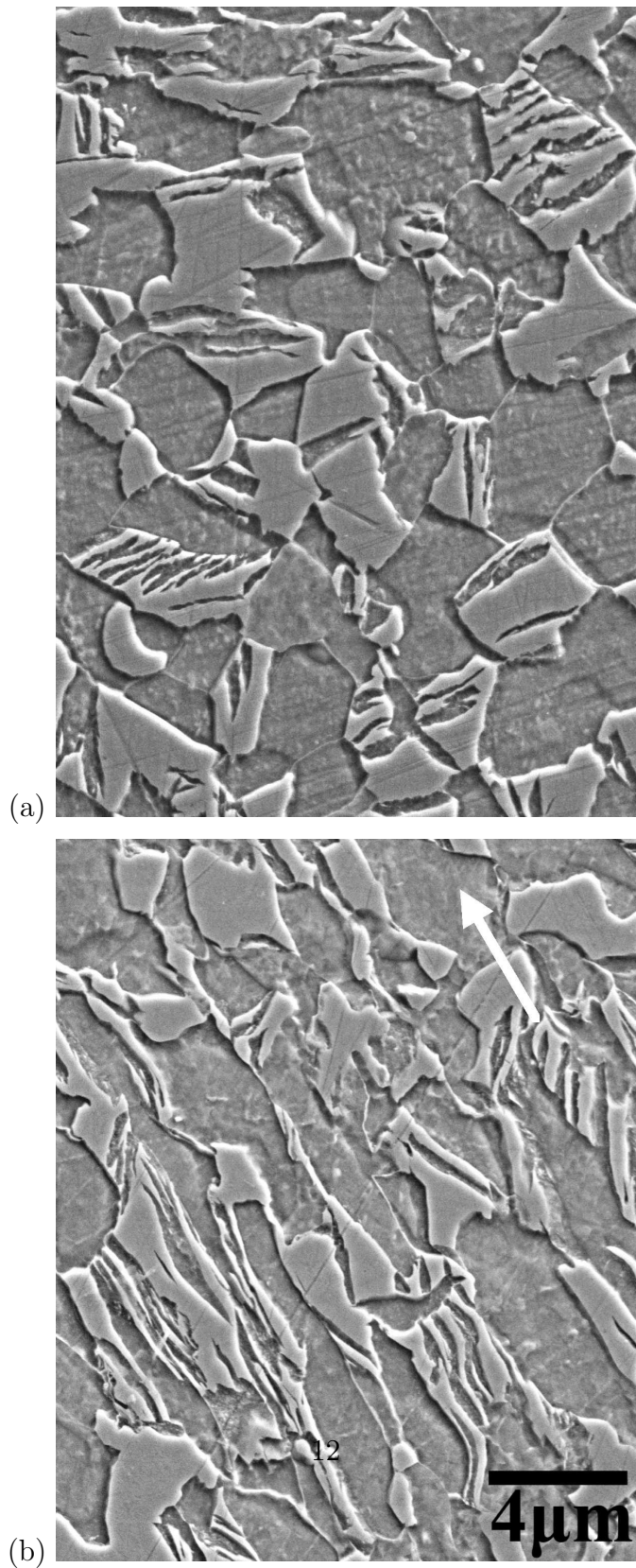


Figure 3: Scanning electron micrographs. (a) Sample prior to deformation. (b) After deformation, in a region within 2 mm off the fracture surface. The tensile axis is identified by the white arrow.

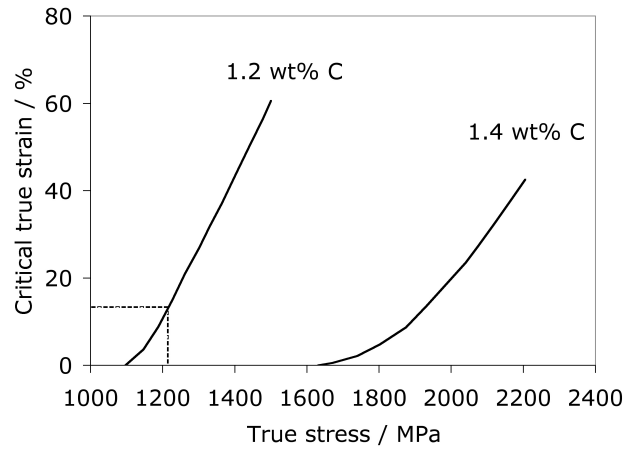


Figure 4: Calculation of the critical value of the true strain required for the onset of mechanical stabilisation, as a function of the maximum true stress experienced by the austenite. The dashed line represents the circumstances for the first tensile test listed in Table 1.

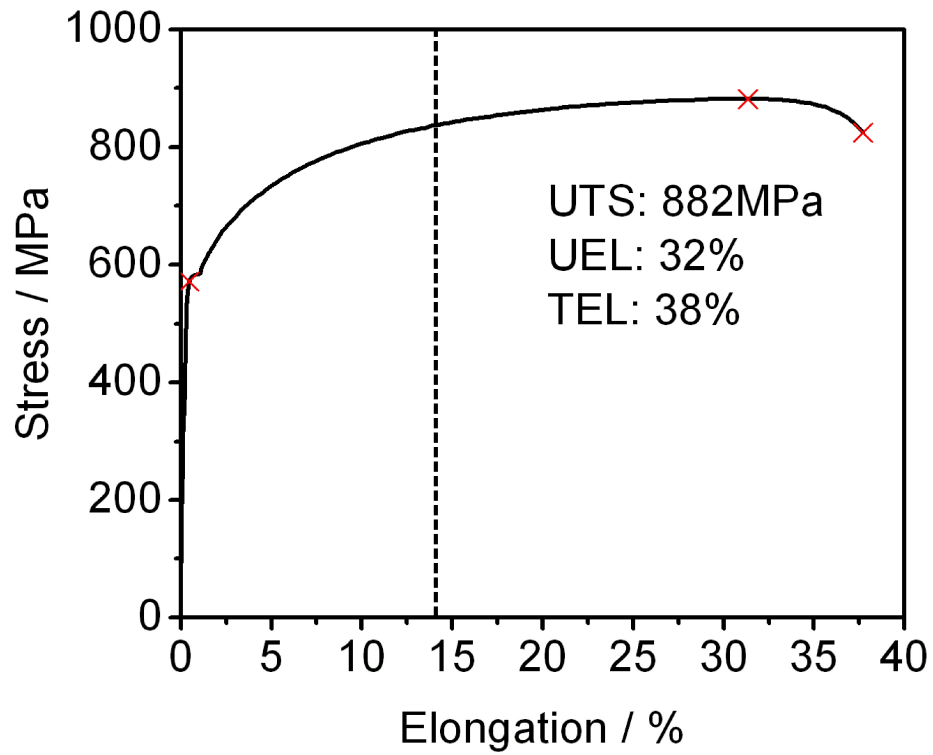


Figure 5: Engineering stress versus engineering strain curve for the first tensile test listed in Table 1. The dashed line represents the critical strain for the onset of mechanical stabilisation. It is fascinating that the work hardening rate is much smaller beyond this strain.

Mechanical Stabilisation of Retained Austenite in δ -TRIP Steel

H. L. Yi^a, K. Y. Lee^b, H. K. D. H. Bhadeshia^{a,c}

^a*Graduate Institute of Ferrous Technology, Pohang University of Science and Technology, Pohang 790-784, Republic of Korea*

^b*POSCO Technical Research Laboratories, Gwangyang-si, Jeonnam, Republic of Korea*

^c*Materials Science and Metallurgy, University of Cambridge, Cambridge CB2 3QZ, U.K.*

Abstract

Recent research suggests that extraordinary combinations of strength and ductility can be achieved in the so-called δ -TRIP steels, which contain ferrite, bainite and austenite. A part of the reason for the ductility of almost 40% elongation at a strength of some 900 MPa, is believed to be the optimal stability of the austenite to plastic deformation. We demonstrate here that mechanical stabilisation plays an important role in preserving the austenite to large plastic strains.

Keywords: TRIP-assisted steel, δ -TRIP, Mechanical stabilisation, Retained austenite

1. Introduction

TRIP-assisted steels, in which the retained austenite undergoes stress or strain-induced transformation into martensite gain tensile ductility because of the associated work hardening, which is responsible for delaying the onset of plastic instability [1–5]. ‘TRIP’ stands for transformation induced plasticity [6] but it is important to realise that the transformation strains themselves are a minor component of the total observed elongation [7]. There have been investigations which suggest that there is an optimum stability necessary for the retained austenite [8–10]. If it decomposes during the early stages of

Email addresses: hityih1@postech.ac.kr (H. L. Yi), (K. Y. Lee), hkdb@cam.ac.uk, corresponding author (H. K. D. H. Bhadeshia)

deformation then it is not able to contribute when significant damage mechanisms initiate. Too high a stability in turn reduces its ability to enhance the work hardening capacity.

The stability of the retained austenite has in the past been considered in terms of two main factors, its chemical composition (primarily the carbon content) [10–12] or its size [13–23]. We show in this work that there is a further contribution, arising from the accumulation of deformation induced defects within the retained austenite, which resist the progress of martensitic transformation by a process known as *mechanical stabilisation* [13, 24–29].

2. Experimental

The alloy design procedure is described elsewhere [30], but was manufactured as a 34 kg ingot with dimensions $100 \times 170 \times 230$ mm using a vacuum furnace. The ingot was reheated to 1200°C for rough rolling to make 25–30 mm slabs followed by air cooling. The slabs were then reheated to 1200°C and hot-rolled with the temperature maintained above 900°C down to 3 mm thickness, followed by cold-rolling to 1.8 mm thick sheet. The final chemical compositions is as follows:



Tensile specimens (ASTM E8M–00) made from the alloy were intercritically annealed at 800°C for 10 min, cooled rapidly by quenching into a salt bath for isothermal transformation at 330°C for 30 min in order to induce the formation of bainitic ferrite; the samples were then air cooled to ambient temperature. The amount of retained austenite and bainitic ferrite in the final microstructure represents the fraction of austenite present at the intercritical annealing temperature; this fraction was found using quantitative metallography to be 0.43 ± 0.04 where the uncertainty represents one standard deviation.

The 1.8 mm thick tensile specimens were strained at $3.3 \times 10^{-3} \text{ s}^{-1}$, with the reported elongations measured over a gauge length of 10 mm. In one case, a tensile sample was, after fracture, subjected to X-ray diffraction at four locations on its length; the locations concerned were separated using an Accutom 50 precision cutter equipped with a 0.5 mm thick alumina cutting disc.

3. Mechanical behaviour and microstructure

Tensile testing revealed that the alloy has an excellent combination of ultimate tensile strength and elongation, with the product of these two quantities coming to $\approx 33,000$ MPa %; data from three such tests are summarised in Table 1 and all three true-stress versus true-strain curves are shown in Fig. 1 in order to illustrate the consistency of strain hardening rates between the specimens. Fig. 3 shows scanning electron micrographs of the structure before and after tensile deformation in the vicinity of the fracture position. The initial structure consists of allotriomorphic ferrite, and equiaxed, blocky regions of retained austenite containing plates of bainitic ferrite which in some cases partition the austenite into films. Fig. 3b shows the remarkable elongation of the austenite islands along the tensile axis; there is no sign of microcracking, which is surprising if the majority of the austenite has transformed into high carbon, untempered martensite.

X-ray experiments interpreted using Reitveld analysis revealed $19.6 \pm 0.2\%$ retained austenite in the initial structure; the carbon concentration (w_C) of the austenite was estimated from the lattice parameter (a_γ in Å) using the relationship due to Dyson and Holmes [31]:

$$\frac{w_C}{0.003} = a_\gamma - 3.578 - 0.00095w_{Mn} - 0.0056w_{Al} - 0.0015w_{Cu} \quad (1)$$

where w stands for the weight percent of the solute identified in the subscript. The concentration of the substitutional solutes specifically in the austenite was measured using energy dispersive X-ray microanalysis (Table 2). A reasonable average value of $w_C \approx 1.33$ wt% was obtained.

Fig. 2 shows that although the austenite does undergo some martensitic transformation during deformation, much of it is retained even at a distance less than about 2 mm away from the point of fracture. This is remarkable given that the plastic elongation recorded over a gauge length of 10 mm is in excess of 37%. In this respect, a re-examination of Fig. 3b shows that the larger blocky regions of austenite seem to have to some extent retained their shape whereas those which are subdivided by bainite plates have elongated. This would be consistent with the well-known effect that blocks of retained austenite are less stable than films [20]. We now proceed to explain why the austenite is reluctant to transform in spite of the large plastic strains involved.

4. Mechanical stabilisation of retained austenite

Martensitic transformation involves the glide of glissile α'/γ interfaces which consist of arrays of dislocations which can move without diffusion. The process is similar to conservative slip except that the structure of the interface leads to a change in crystal structure as it translates into the austenite [32]. Any obstacles in the path of the interface therefore hinder its motion, precisely in the same manner that slip dislocations are hindered by barriers such as forest dislocations. There comes a point where the density of barriers present in the austenite becomes so large that the driving force for the growth of martensite becomes inadequate compared with that which obstructs the interface. This defines the onset of mechanical stabilisation whence martensitic transformation ceases. This concept forms the basis of a quantitative model for predicting mechanical stabilisation when displacive transformations occur in austenite which is plastically deformed.

Mechanical stabilisation occurs when the stress driving (τ_T) the interface equals that opposing its motion, $\tau + \tau_S$, where τ is the resistance from dislocation debris in the austenite, and τ_S the contribution from solid-solution strengthening of austenite [33]:

$$\begin{aligned} \tau_T &= \tau + \tau_S \\ \text{so that } b\Delta G &= \frac{1}{8\pi(1-\nu)}Gb^{\frac{3}{2}}\sqrt{\frac{\epsilon}{L}} + \tau_S b \end{aligned} \quad (2)$$

where ϵ is the plastic strain, b is the magnitude of the Burgers vector of the dislocations involved, ΔG is the free energy change driving the motion of the interface, G is the shear modulus of the austenite and ν is its Poisson's ratio. L is the average distance moved by the dislocations and $L = \delta D/(\delta + D\epsilon)$ where D is the original grain size of austenite before straining, and δ is a coefficient equal approximately to $1\ \mu\text{m}$ [34].

The original model considered transformation from deformed austenite which was not otherwise under the influence of an external stress. The present work involves tensile deformation so it is appropriate to include a mechanical free energy contribution to the driving force for martensitic transformation, and as in the earlier work, to reduce the total chemical free energy available by the stored energy of martensite ($600\ \text{J mol}^{-1}$, [35]):

$$\Delta G = \Delta G_{\text{CHEM}} + \Delta G_{\text{MECH}} - 600\ \text{J mol}^{-1} \quad (3)$$

The chemical driving force for transformation, $\Delta G_{\text{CHEM}} = \Delta G_{\gamma} - \Delta G_{\alpha}$ was calculated using MTDATA combined with TCFE (1.21 version) database [36] at 20 °C, assuming the chemical composition of the austenite as listed in Table 2 and for two different carbon concentrations (1.2 and 1.4 wt%) rather than the average 1.33 wt% determined from the X-ray experiments. This is because larger regions of austenite are expected to contain relatively less carbon [11].

The mechanical component of the free energy change is given by $\Delta G_{\text{MECH}} = \sigma \times 0.86 \text{ J mol}^{-1}$ [37, 38], where σ is the external stress experienced by the austenite. The complete set of parameters used in the calculations is listed in Table 3.

Fig. 4 shows the calculations of the critical value of true strain required to trigger mechanical stabilisation, as a function of the maximum value of the true tensile stress experienced by the retained austenite. The stress assists martensitic transformation which means that mechanical stabilisation is triggered at ever larger values of the critical strain as the stress increases. The two curves represent two different carbon concentrations, the lower value assumed to be that corresponding to the blocks of austenite and the 1.4 wt% representing the film type austenite. They also differ in their grain sizes as listed in Table 3. The critical strain is zero, *i.e.*, transformation simply does not occur, if the stress is less than 1096 MPa in the case of the 1.2 wt% austenite, and 1631 MPa for the 1.4 wt% austenite.

The dashed vertical line represents the actual true stress to which the austenite is subjected for the tensile test data listed in Table 1, suggesting that mechanical stabilisation occurs when the austenite is deformed to a true strain of 13%; this corresponds to an engineering strain of about 14%, which is much smaller than the total elongation of 37%. This means that the austenite can transform only during the period of the initial strain, after which it becomes stabilised. The data presented in Fig. 2 support this conclusion. Furthermore, it is only the blocky austenite which is presumed to be leaner in carbon that can undergo transformation, consistent with the fact that the blocks show less elongation in micrographs than the film type austenite (Fig. 3). They would essentially cease to deform once hard, untempered, high-carbon martensite forms.

The implications of this interpretation are interesting, that the initial transformation helps enhance the work hardening capacity, but further ductility is maintained by austenite which deforms in a way that is approximately compatible with the overall microstructure. Indeed, Fig. 5 shows the stress–

strain relationship for one of the samples confirms that the work hardening rate diminishes significantly as the critical strain of 14% is approached.

5. Conclusions

A TRIP-assisted steel which exhibits substantial ductility contains austenite, the coarser regions of which transform during the early stages of deformation but the remainder is in a state which is mechanically stabilised and hence remains untransformed until the point of fracture. Thus, regions of austenite can be observed to elongate with the majority phase which is ferrite. A published theory for the mechanical stabilisation of the austenite has been adapted to provide a quantitative basis for assessing the onset of mechanical stabilisation when the austenite is not only contains deformation debris but is also under a state of mechanical stress.

Acknowledgments

We are grateful to Professor Hae-Geon Lee for laboratory facilities at GIFT, and to POSCO for the Steel Innovation Programme. Support from the World Class University Programme of the National Research Foundation of Korea, Ministry of Education, Science and Technology, project number R32-2008-000-10147-0 is gratefully acknowledged.

References

- [1] O. Matsumura, Y. Sakuma, H. Takechi: Transactions of the Iron and Steel Institute of Japan 27 (1987) 570–579.
- [2] O. Matsumura, Y. Sakuma, H. Takechi: Scripta Metallurgica 27 (1987) 1301–1306.
- [3] Y. Sakuma, O. Matsumura, H. Takechi: Metallurgical & Materials Transactions A 22 (1991) 489–498.
- [4] P. J. Jacques: Current Opinion in Solid State and Materials Science 8 (2004) 259–265.
- [5] B. DeCooman: Current Opinion in Solid State and Materials Science 8 (2004) 285–303.

- [6] W. W. Gerberich, G. Thomas, E. R. Parker, V. F. Zackay: Metastable austenites: decomposition and strength: in: Second International Conference on Strength of Metals and Alloys: ASM International, Ohio, USA, 1970: pp. 894–899.
- [7] H. K. D. H. Bhadeshia: ISIJ International 42 (2002) 1059–1060.
- [8] K. Sugimoto, N. Usui, M. Kobayashi, S. Hashimoto: ISIJ International 32 (1992) 1311–1318.
- [9] K. Sugimoto, M. Kobayashi, S. Hashimoto: Metallurgical Transactions A 23A (1992) 3085–3091.
- [10] C. Garcia-Mateo, F. G. Caballero: Materials Transactions 46 (2005) 1839–1846.
- [11] A. Itami, M. Takahashi, K. Ushioda: ISIJ International 35 (1995) 1121–1127.
- [12] Y. Sakuma, O. Matsumura, O. Akisue: ISIJ International 31 (1991) 1348–1353.
- [13] W. C. Leslie, R. L. Miller: ASM Transactions Quarterly 57 (1964) 972–979.
- [14] D. Duchateau, M. Guttman: Acta Metallurgica 29 (1981) 1291–1297.
- [15] M. Umemoto, W. S. Owen: Metallurgical Transactions 5 (1974) 2041–2046.
- [16] G. S. Ansell, P. J. Brofman, T. J. Nichol, G. Judd: Effect of austenite strength on the transformation to martensite in Fe–Ni and Fe–Ni–C alloys: in: G. B. Olson, M. Cohen (Eds.), International Conference on Martensitic Transformations ICOMAT '79: 1979: pp. 350–355.
- [17] P. J. Brofman, G. S. Ansell: Metallurgical Transactions A 14A (1983) 1929–1931.
- [18] S. J. Lee, Y. K. Lee: Materials Science Forum 475–479 (2005) 3169–3172.

- [19] J. Huang, Z. Xu: *Materials Science & Engineering A* A438–440 (2006) 254–257.
- [20] H. K. D. H. Bhadeshia, D. V. Edmonds: *Metal Science* 17 (1983) 411–419.
- [21] H. K. D. H. Bhadeshia, D. V. Edmonds: *Metal Science* 17 (1983) 420–425.
- [22] B. V. N. Rao, M. S. Rashid: *Metallography* 16 (1983) 19–37.
- [23] F. G. Caballero, C. G. Mateo, J. Chao, M. J. Santofimia, C. Capdevila, C. G. de Andrés: *ISIJ International* 48 (2008) 1256–1262.
- [24] E. S. Machlin, M. Cohen: *Trans. Metall. Soc. AIME* 191 (1951) 746–754.
- [25] H. C. Fiedler, B. L. Averbach, M. Cohen: *Transactions of the American Society for Metals* 47 (1955) 267–290.
- [26] J. R. Strife, M. J. Carr, G. S. Ansell: *Metallurgical Transactions A* 8A (1977) 1471–1484.
- [27] V. Raghavan: *Kinetics of Martensitic Transformations*: eds G. B. Olson and W. S. Owen, ASM International, Ohio, US, 1992: Ch. 11: pp. 197–226.
- [28] K. Tsuzaki, S. Fukasaku, Y. Tomota, T. Maki: *Trans. JIM* 32 (1991) 222–228.
- [29] H. K. D. H. Bhadeshia: *Materials Science & Engineering A* 273–275 (1999) 58–66.
- [30] H. L. Yi, K. Y. Lee, H. K. D. H. Bhadeshia: *Proceedings of the Royal Society A* 467 (2010) 234–243.
- [31] D. J. Dyson, B. Holmes: *Journal of the Iron and Steel Institute* 208 (1970) 469–474.
- [32] J. W. Christian: *Theory of Transformations in Metal and Alloys, Part II*: 3rd Edition: Pergamon Press, 2003.
- [33] S. Chatterjee, H. S. Wang, J. R. Yang, H. K. D. H. Bhadeshia: *Materials Science and Technology* 22 (2006) 641–644.

- [34] F. Barlat, M. V. Glazov, J. C. Brem, D. J. Lege: Canadian Metallurgical Quarterly 18 (2002) 919–939.
- [35] J. W. Christian: Thermodynamics and kinetics of martensite: in: G. B. Olson, M. Cohen (Eds.), International Conference on Martensitic Transformations ICOMAT '79: 1979: pp. 220–234.
- [36] NPL: MTDATA: Software, National Physical Laboratory, Teddington, U.K. (2006).
- [37] S. Denis, E. Gautier, A. Simon, G. Beck: Materials Science and Technology 1 (1985) 805–814.
- [38] G. B. Olson: Transformation plasticity and the stability of plastic flow: in: Deformation, Processing and Structure: American Society for Metals, Metals Park, Ohio, USA, 1982: pp. 390–424.

Table 1: The results of three tensile tests. The terms YS, UTS and TEL stand for yield strength, ultimate tensile strength and total elongation, respectively.

YS /MPa	UTS /MPa	UEL /%	TEL /%	UTS \times TEL / MPa%
573	882	31	38	33,247
541	880	31	37	32,940
536	894	31	37	32,691

Table 2: Alloying element distribution in phases in heat-treated specimens, wt%.

Phase	Al	Si	Mn	Cu
γ	2.56 \pm 0.14	0.32 \pm 0.08	1.87 \pm 0.17	0.55 \pm 0.13
α	3.13 \pm 0.05	0.40 \pm 0.06	1.15 \pm 0.05	0.44 \pm 0.06

Table 3: Parameters used for the modelling in blocky and lath type of austenite.

	D / m	C / wt%	G / Pa	ν	b / m	$\tau_s b /$ N m $^{-1}$	ΔG_{Chem} / J mol $^{-1}$
Blocky	5 \times 10 $^{-6}$	1.2	8 \times 10 10	0.27	2.52 \times 10 $^{-10}$	0.057640	1281
Film	0.5 \times 10 $^{-6}$	1.4	8 \times 10 10	0.27	2.52 \times 10 $^{-10}$	0.06644	1080

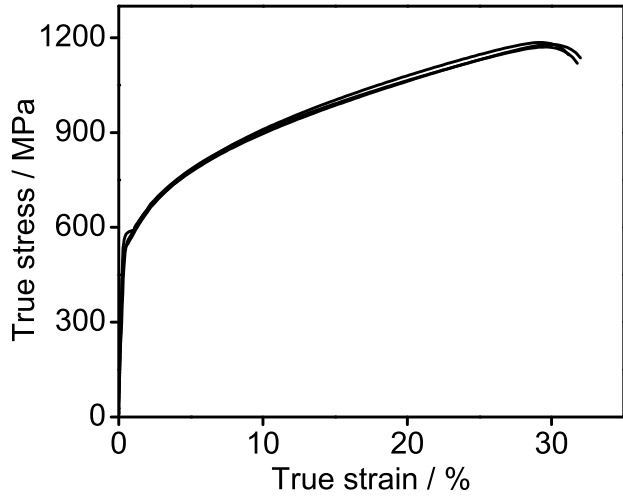


Figure 1: Superimposed true-stress versus true-strain curves for the three tensile tests.

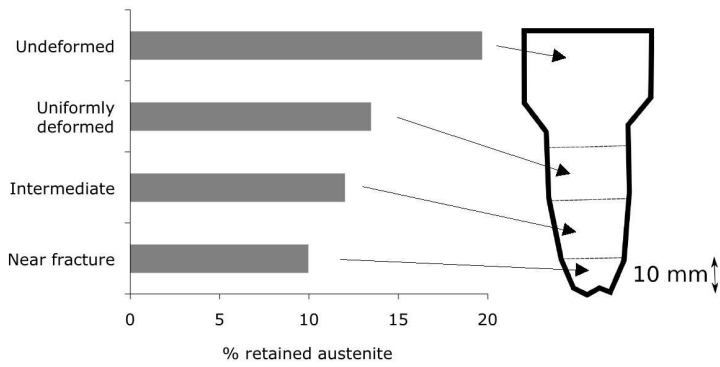


Figure 2: Retained austenite in different regions relative to the fracture surface. The point marked 'Fracture' is within 2 mm of the fracture surface.

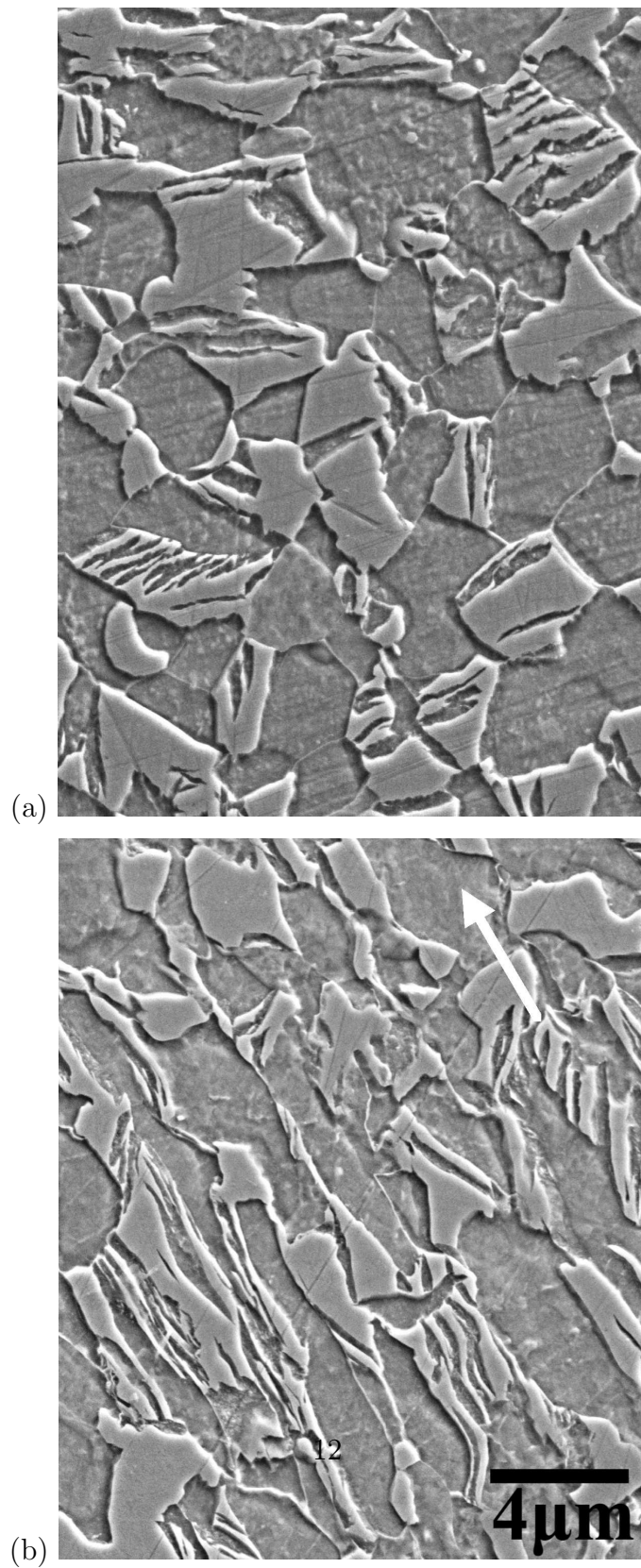


Figure 3: Scanning electron micrographs. (a) Sample prior to deformation. (b) After deformation, in a region within 2 mm off the fracture surface. The tensile axis is identified by the white arrow.

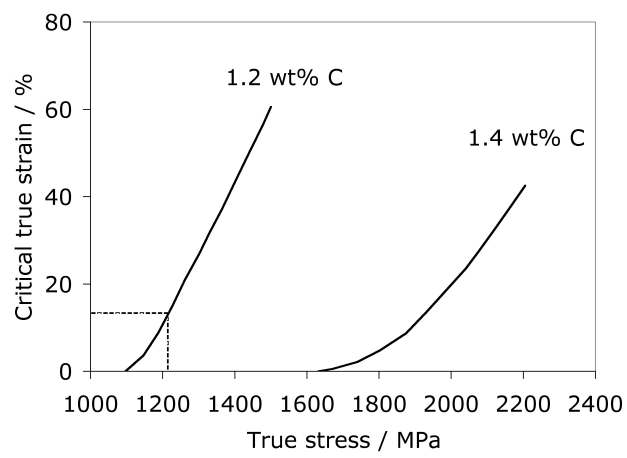


Figure 4: Calculation of the critical value of the true strain required for the onset of mechanical stabilisation, as a function of the maximum true stress experienced by the austenite. The dashed line represents the circumstances for the first tensile test listed in Table 1.

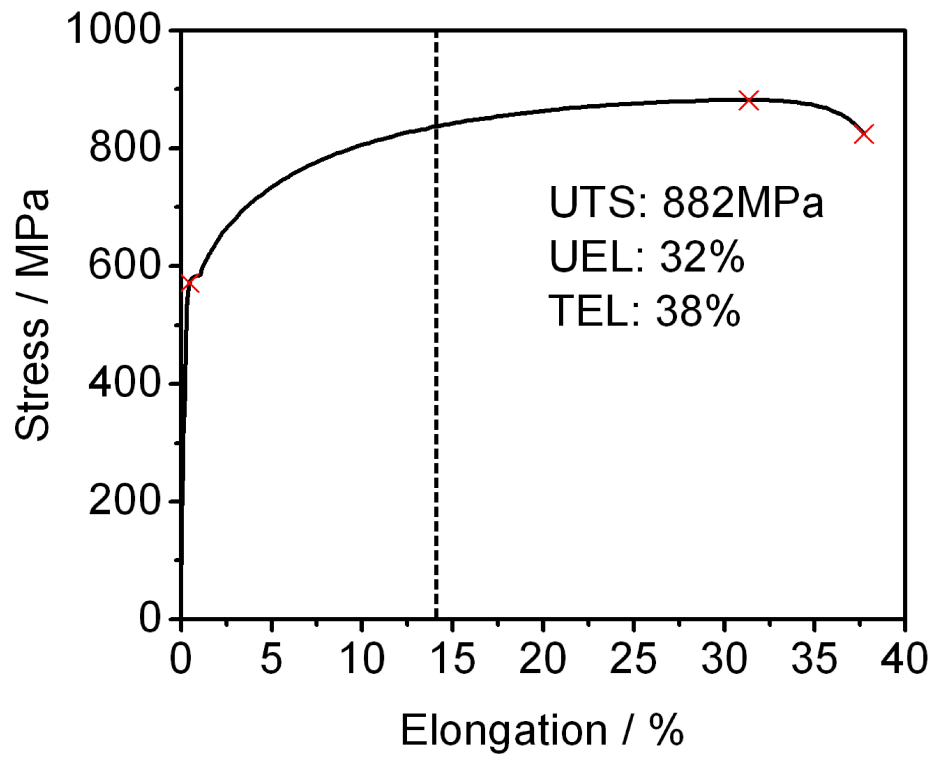


Figure 5: Engineering stress versus engineering strain curve for the first tensile test listed in Table 1. The dashed line represents the critical strain for the onset of mechanical stabilisation. It is fascinating that the work hardening rate is much smaller beyond this strain.